The Astrophysical Journal, 614:135–141, 2004 October 10

UNVEILING THE CENTRAL PARSEC REGION OF AN ACTIVE GALACTIC NUCLEUS: THE CIRCINUS NUCLEUS IN THE NEAR-INFRARED WITH THE VERY LARGE TELESCOPE

M. Almudena Prieto,[1] K. Meisenheimer,[1] Olivier Marco,[2] Juha Reunanen,[3] Marcella Contini,[4] Y. Clenet,[5] R. I. Davies,[6] D. Gratadour,[5] Th. Henning,[1] U. Klaas,[1] J. Kotilanien,[3] Ch. Leinert,[1] D. Lutz,[6] D. Rouan,[5] and N. Thatte[7]

Received 2004 March 24; accepted 2004 June 11

ABSTRACT

VLT J- to M'-band adaptive optics observations of the Circinus galaxy on parsec scales resolve a central bright K_s-band source with a FWHM size of 1.9 ± 0.6 pc. This source is only visible at wavelengths longward of 1.6 μm and coincides in position with the peak of the [Si VII] 2.48 μm coronal line emission. With respect to the peak of the central optical emission, the source is shifted by $\sim$0.″15 (2.8 pc) to the southeast. Indeed, the K_s-band source defines the vertex of a fairly collimated beam that extends for $\sim$10 pc and is seen in both continuum light shortward of 1.6 μm and in Hα line emission. The source also lies at the center of a $\sim$19 pc size [Si VII] ionization bicone. Identifying this source as the nucleus of Circinus, its size is compatible with a putative parsec-scale torus. Its spectral energy distribution, characterized by a prominent narrow peak, is compatible with a dust temperature of 300 K. Hotter dust within a 1 pc radius of the center is not detected. The active galactic nucleus (AGN) luminosity required to heat this dust is in the range of X-ray luminosities that have been measured toward the central source. This in turn supports the existence of highly obscuring material, with column densities of 10^{24} cm^{-2}, that must be located within 1 pc of the core.

Subject headings: galaxies: individual (Circinus) — galaxies: nuclei — galaxies: Seyfert — infrared: galaxies

1. INTRODUCTION

Circinus is the second-closest active galactic nucleus (AGN; $\sim$4 Mpc, Freeman et al. 1977; $1'' \sim 19$ pc) in the Southern Hemisphere after Centaurus A. It is an SA(s)b galaxy inclined by $\sim$65° with a Seyfert type 2 AGN at its center. Several dust lanes running north to south across the galaxy hide a large fraction of its eastern side. Probably for this reason, Circinus shows a one-sided cone of ionized gas that extends to the northwest in Hα and [O III] images on kiloparsec scales (Marconi et al. 1994) and in X-rays on smaller scales (Smith & Wilson 2001). The hard 1–100 keV X-ray spectrum indicates the presence of an obscured nucleus with $N(\mathrm{H}) \sim 4 \times 10^{24}$ cm^{-2} (Matt et al. 1999). The highest spatial resolution view of its central region comes from VLBI maps of H_2O maser emission (Greenhill et al. 2003). The H_2O emission is interpreted in terms of a central edge-on Keplerian disk with inner and outer radii of 0.1 and 0.4 pc, respectively, and outflowing material up to 1 pc from the center.

This paper presents near-to-diffraction–limited images of the Circinus galaxy in the 1.2–5 μm range observed with the adaptive optics assisted imaging spectrograph NACO at the VLT. Circinus was observed as part of the multiresolution imaging program ZIDNAG (Zooming Into Dusty Nuclei of Active Galaxies) aimed at imaging the dusty tori in the closest AGN with both NACO and, subsequently, VLTI observations at 10 and 2.2 μm.

The physical scales associated with the spatial resolution of the Circinus images presented in this paper lie in the range 1.5–3 pc, hence probing the presence and dimensions of obscuring material (the putative torus) around this type 2 AGN.

[1] Max-Planck-Institut für Astronomie, Königstuhl 17, Heidelberg D-69117, Germany; prieto@mpia.de.
[2] European Southern Observatory Paranal, Santiago, Chile.
[3] Tuorla Observatory, University of Turku, Piikkiö, Finland.
[4] School of Physics and Astronomy, Tel-Aviv University, Tel-Aviv 69978, Israel.
[5] Observatoire de Paris, France.
[6] Max-Planck-Institut für extraterrestrische Physik, Garching, Germany.
[7] University of Oxford, UK.

2. OBSERVATIONS AND ANALYSIS

NACO images in broad J (1.3 μm), K_s (2.2 μm), L' (3.8 μm), and M' (4.8 μm) bands and in narrow 2.42 μm and 2.48 μm bands were obtained with the UT4 unit telescope of the VLT in 2003 May (broadband) and 2003 March (narrowband). With the exception of the M'-band image, which was taken in chopping mode and has a reduced field of view of $12'' \times 12''$, all the images have a field of view of $27'' \times 27''$ and a pixel scale of 0.″027 per pixel. The pixel scale fully samples the diffraction limit of the VLT in the K_s, L', and M' bands but undersamples it at J. The wavelength of the narrowband image at 2.48 μm is centered on the position of the coronal [Si VII] 2.48 μm line; the image at 2.42 μm is an off-line image taken for continuum subtraction.

The optical wave-front sensor was used for all wavelengths. Final images were made after sky-subtracting, shifting, and co-adding a number of raw frames (about 30 in J and K_s; 170 and 90 in L' and M', respectively) taken at random dithered positions within a jitter box of $\sim$20″ around the central position of Circinus. The large number of raw frames and the size of the jitter width proved to be a robust procedure for generating reliable sky images from the science frames themselves without resorting to separate observations of the sky. Exposure times ranged from 3 minutes in J and K_s and 5 minutes in L' to 10 minutes in M' and 20 minutes in the narrowband filters.

The resulting FWHM spatial resolutions were measured from several stars in the field of the science frames to be $0.''21 \pm 0.''01$ in the J band, $0.''16 \pm 0.''02$ in the K_s band, $0.''20 \pm 0.''01$ at 2.42 μm, and $0.''19 \pm 0.''01$ at 2.48 μm. In the L' and M' bands, resolutions of $<0.''12$ and $<0.''13$, respectively, were derived from star images taken after the Circinus observations. The Strehl values achieved are difficult to assess, as the Circinus nucleus is extended, and the stars in the science frame that could be used for that purpose are immersed in the galaxy light. Nevertheless, for orientational purposes, the Strehl values measured in real time by the adaptive optic system are provided: $\sim$20% in J, 15% in K_s, and between 40% and 50% in the L'- and M'-band images.

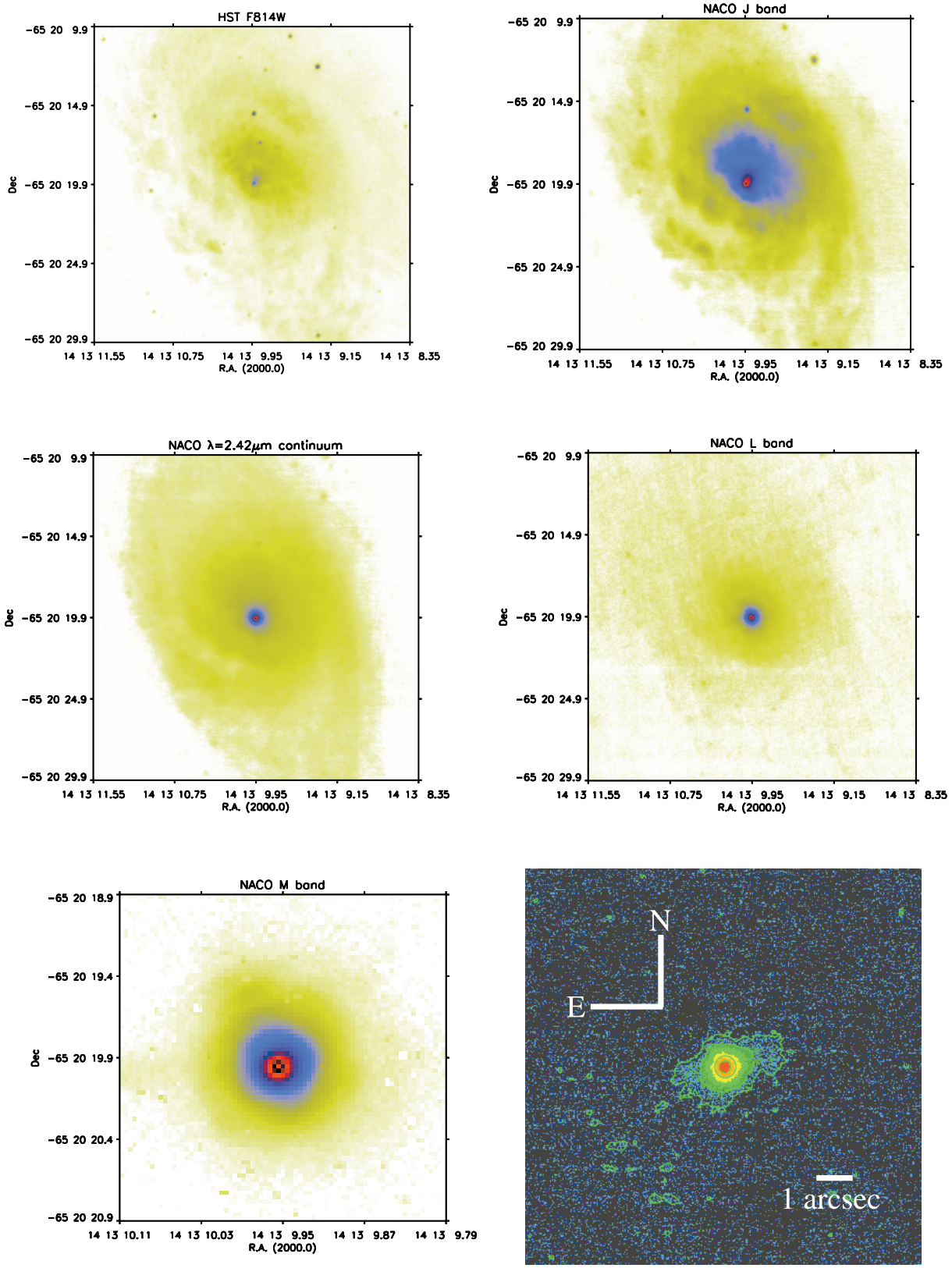

FIG. 1.—*HST* and NACO images of the central $20'' \times 20''$ region of Circinus ($2\farcs5 \times 2\farcs5$ in M' band): *top left*, F814W (8140 Å) WFPC2-PC chip; *top right*, J band; *center left*, 2.42 μm; *center right*, L' band; *bottom left*, M' band; *bottom right*, pure coronal [Si VII] 2.48 μm line emission.

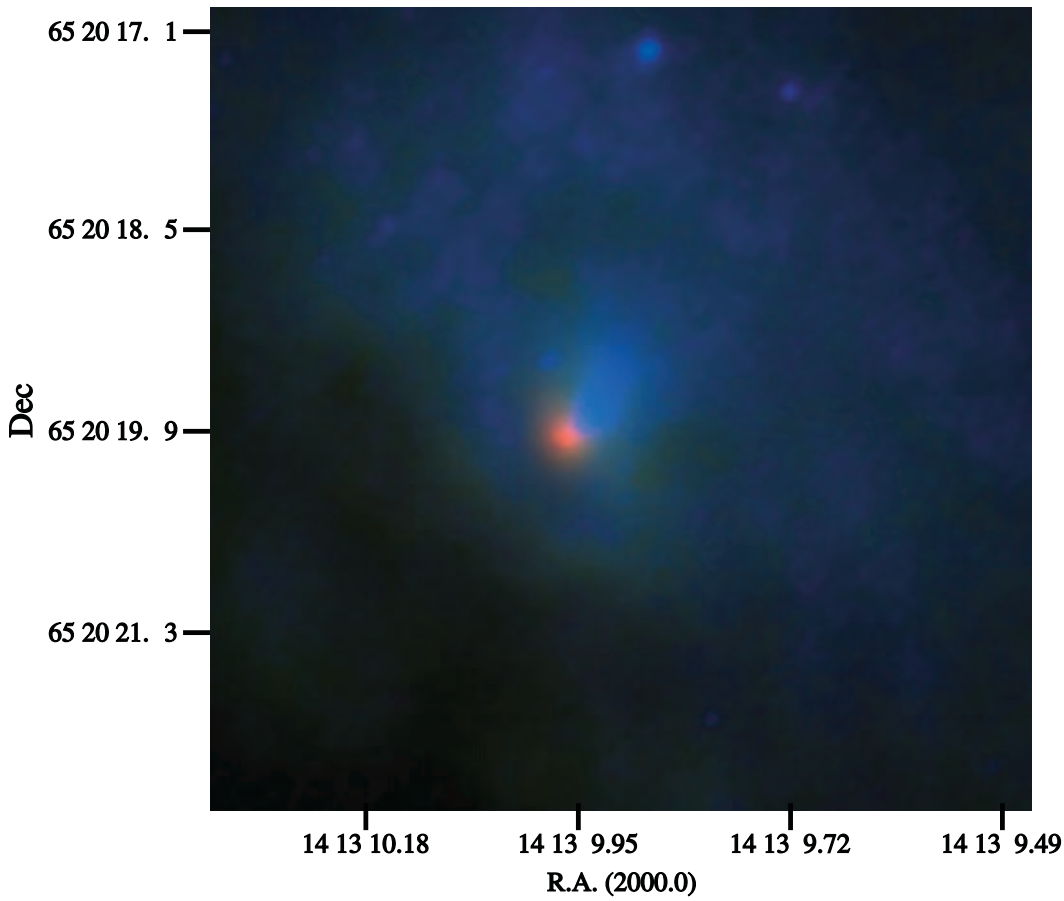

FIG. 2.—True-color image combining *HST* WFPC2-PC F814W (*blue*) and NACO J (*green*) and K_s (*red*) bands. The figure shows the 10 pc collimated beam (to which only the optical and J band contribute) pointing away from the bright central source (comprising only the K_s-band emission), which we argue is the nucleus.

For comparison purposes, Wide Field Planetary Camera 2 (WFPC2) broadband 8140 Å (F814W, PC chip only) and Hα images, as well as Near-Infrared Camera and Multi-Object Spectrometer (NICMOS) H-band (F160W) and 1.66 μm narrowband images, were retrieved from the *Hubble Space Telescope* (*HST*) archive.

Figure 1 presents a compilation of the most relevant images from the *HST* F814W to the NACO M' broadband images and a [Si VII] 2.48 μm "pure" line emission image. The H, K_s, and 2.48 μm images resemble the 2.42 μm image that already appears in Figure 1 and thus are not shown. The morphology of Circinus does not change at wavelengths shortward of 1.6 μm. However, at longer wavelengths, its eastern side, which is largely hidden by dust lanes in the F814W and J-band images, is progressively revealed. In the L' and M' bands, Circinus is reduced to a more compact region (total diameter $\sim$1.″2) with very faint (signal-to-noise ratio [S/N] $\sim$3, 6 mag fainter than the peak) extended emission in L'. This is due to a combination of lower efficiency of the NACO camera and the natural decrease in stellar flux at these wavelengths.

3. ASTROMETRY OF THE INFRARED CENTRAL SOURCE

Astrometric registration of the *HST* F814W and NACO images was achieved thanks to the presence of several stars common to all images. For this purpose, the F814W PC image scale of 0.″04 per pixel was rebinned to that of NACO. Based on the registration of 6–7 stars in the field, an accuracy better than $\pm$1 pixel was reached between the F814W, J, K_s, 2.42 μm, and 2.48 μm images. An accuracy of about $\pm$2 pixels was reached for the L'-band image, for which only one star was available. No registration was possible for the M'-band image.

Following registration, it was found that the central peaks of the F814W and J-band images coincided spatially. Their position, however, is offset by $\sim$0.″15 (2.8 pc) northwest with respect to the central peak position found in all of the K_s, 2.42 μm, 2.48 μm, and L' images and in the F160W image. The morphology of the central emission is very different in the two cases. The central emission in the F814W and J-band images appears diffuse and rather collimated over a distance of $\sim$0.″6 (10 pc) along the inner main axis of Circinus' ionization cone (see the *HST* Hα image in Wilson et al. 2000). Close examination of the 1.66 μm narrowband "continuum" image shows a similar morphology, although with less definition. On the other hand, the K_s, 2.42 μm, 2.48 μm, and L' images show a bright compact source located at the southeast apex of the collimated beam seen in the F814W and J-band images (Fig. 2).

The position of the infrared source also coincides with the peak emission of the (pure) [Si VII] 2.48 μm coronal line. Furthermore, the [Si VII] 2.48 μm exhibits an elongated structure (19 pc radius) extended on both sides of the nucleus (Fig. 1). The direction of the extended emission is not exactly along the main axis of the ionization cone, but it is certainly within the cone boundaries as defined at its base, as apparent from a comparison of Figures 1 and the Hα ionization cone shown in the contours in Figure 3. Thus, it appears that the [Si VII] 2.48 μm emission, which is considerably less affected by extinction than Hα, unveils the countercone of Circinus. This result confirms the

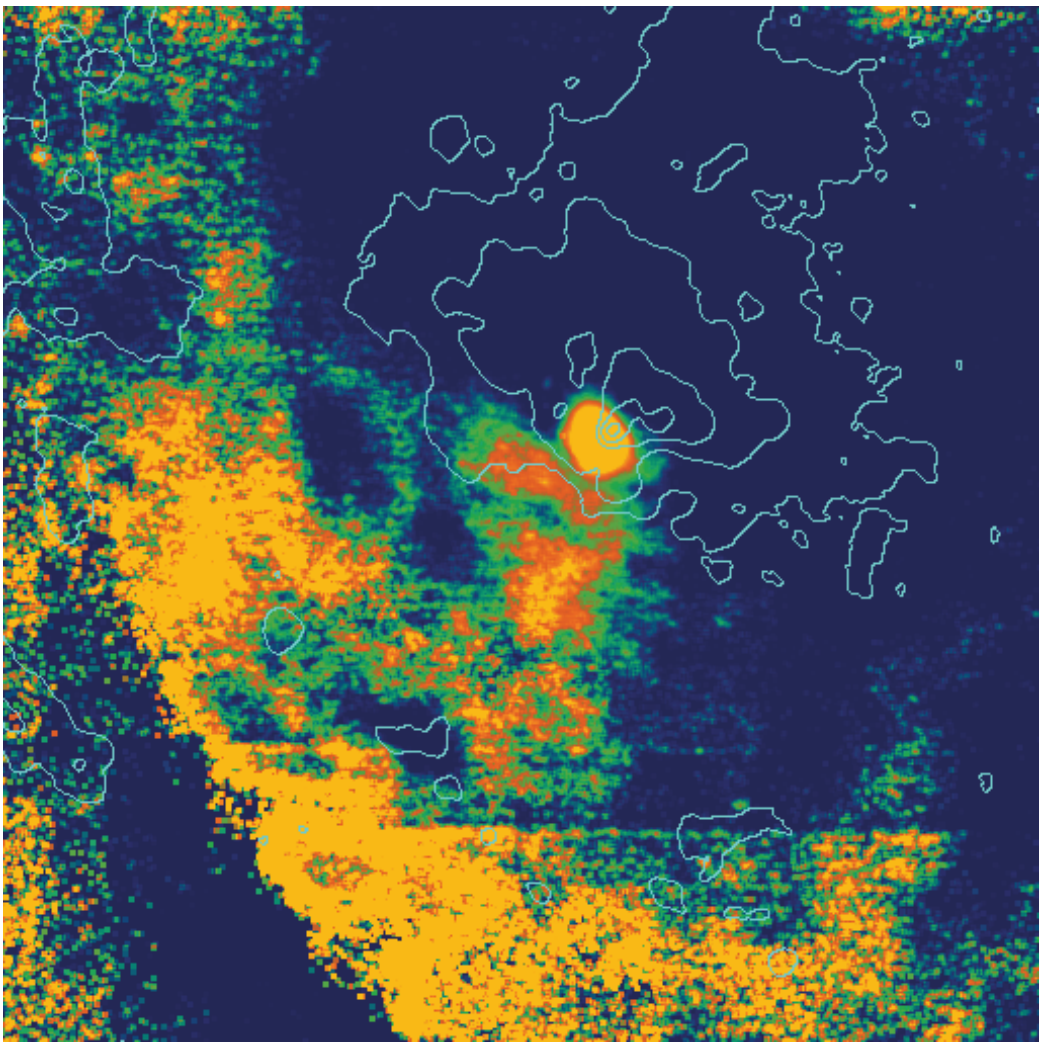

FIG. 3.—NACO [J–2.42 μm] color image. The field of view is $20'' \times 20''$, centered on the nucleus. North is up and east is left. The superimposed contours trace the *HST* Hα emission. This shows Circinus' one-sided ionization cone to the northwest as well as some of the brightest star-forming regions from Circinus' circumnuclear ring, which coincide with regions of lower extinction, in the eastern and southern parts of the galaxy.

report of Maiolino et al. (2000) of countercone emission seen at rather low S/N in the [Si VI] 1.96 μm line. Since [Si VII] 2.48 μm probes Circinus' ionizing continuum at energies of about 200 eV, and considering the symmetric morphology of the emission, it is reasonable to conclude that the central peak of [Si VII] emission pinpoints the active nucleus in Circinus.

Appraising all the evidence above, it appears that the infrared central source detected at wavelengths longer than 1.6 μm qualifies as the true nucleus of Circinus. At this location there is no enhanced emission in the F814W or J-band images, indicating that this infrared central source is fully obscured at wavelengths $\lesssim$1.3 μm.

An attempt to establish the absolute astrometry of the infrared central source was performed on the *HST* F814W image (PC chip) with the USNO star catalog. Based on the *HST* F814W pointing alone, the position of the NACO K_s-band central source is found to be $14^{\rm h}13^{\rm m}9\overset{\rm s}{.}96 \pm 0\overset{\rm s}{.}02 - 65^\circ 20' 19\overset{''}{.}91 \pm 0\overset{''}{.}01$ (with the uncertainties given here derived solely from the relative astrometry of the two images). For the *HST* NICMOS F160W pointing, the position in right ascension is found to be the same, but the declination is offset to the south by 0$\overset{''}{.}$44. For several stars identified in the *HST* F814W image (it was not possible to locate any stars in the F160W image common to the USNO catalog), the difference between the coordinates from the *HST* data and those given in the USNO catalog were found to be smaller than the errors reported for the USNO stars themselves, which were typically 0$\overset{''}{.}$9 on each axis. We therefore assign an uncertainty of 0$\overset{''}{.}$9 to the absolute position derived using the *HST* F814W (PC chip) astrometry. Thus, we find that the position of the Circinus infrared source differs from the maser position derived from the VLBI (Greenhill et al. 2003), which is $14^{\rm h}13^{\rm m}9\overset{\rm s}{.}95 \pm 0\overset{\rm s}{.}02 - 65^\circ 20' 21\overset{''}{.}2 \pm 0\overset{''}{.}1$ (2000.0), by 1$\overset{''}{.}$2, an additional 0$\overset{''}{.}$3 beyond our assigned error. On the other hand, it is consistent with the 2MASS K_s-band position $14^{\rm h}13^{\rm m}9\overset{\rm s}{.}92 - 65^\circ 20' 21\overset{''}{.}57$ (quoted uncertainties are approximately 0$\overset{''}{.}$1). Thus, a clear negative shift in declination applies to all the above optical/infrared positions with respect to the VLBI one. This offset may be related to an intrinsic systematic shift between the radio and optical/infrared coordinate reference systems. But if it were real, it could indicate that the maser source does not actually pinpoint the nucleus but is instead part of the nuclear H_2O outflow measured by Greenhill et al. (2003).

4. NATURE OF THE INFRARED CENTRAL SOURCE

The morphology of the infrared central source in Circinus is rather pointlike at wavelengths longward of 1.6 μm; its FWHM,

TABLE 1
PHOTOMETRY OF CIRCINUS

Band	Magnitude	Flux (mJy)	Aperture Diameter (arcsec)
J	15	$\lesssim$1.6	0.38
H	13.4	4.77	0.1
K	11.4	19	0.38
2.42 μm	10.56	31	0.38
L	7.1	380	0.38
M	4.8	1900	0.38
N	...	9700	1.0
[Si VII] 2.48 μm	...	2.0×10^{-13} ergs cm^{-2} s^{-1}	2.9

NOTE.—All data are from NACO except N band from ESO/TIMMI2 (H. Heijligers 2003, private communication) and H band from *HST*/NICMOS (Quillen et al. 2001).

however, is larger than that of the stars measured in the same images. The size is best determined in the K_s band and, after quadrature subtraction of the resolution beam, is found to have a FWHM $0\farcs11 \pm 0\farcs03$ (1.9 $\pm$ 0.6 pc). In the L' and M' bands, the core sizes are (not deconvolved) FWHM $0\farcs185 \pm 0\farcs05$ and $0\farcs165 \pm 0\farcs05$, respectively.

In Table 1, the nuclear NACO fluxes in apertures of $0\farcs19$ radius, chosen to be about twice the resolution achieved in the K_s band, are provided. The core fluxes from the NICMOS H-band and ESO/TIMMI2 N-band data in apertures less than $1''$ are also included. Figure 4 (*squares*) shows the corresponding infrared spectral energy distribution (SED) complemented by X-ray data from *ROSAT* (1 keV flux; Brinkmann et al. 1994) and *BeppoSAX* (10 keV flux, derived from the absorption-corrected nuclear luminosity $F_{2-10\ \mathrm{keV}} = 3.4 \times 10^{41}$ ergs s^{-1}; Matt et al. 1999) and by radio data at various wavelengths and in different apertures from the compilation of Contini et al. (1998). All the infrared measurements are associated with Circinus' central infrared source except for the J band, since the source is not detected shortward of this wavelength. For consistency, the J-band value given is the integrated flux within an aperture of radius $0\farcs19$ measured at the position of the infrared source.

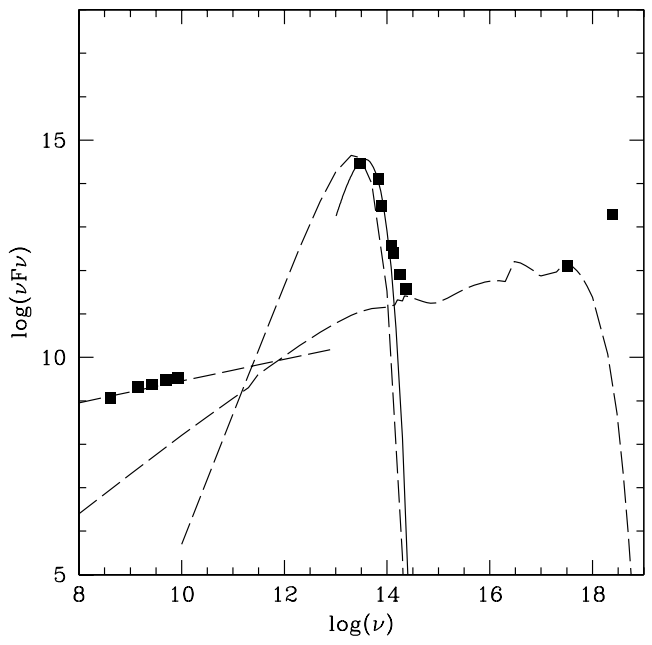

FIG. 4.—SED of Circinus' nucleus. The new infrared data (in the range $\log \nu = 13.5-14.5$) are from Table 1. Note that the J-band flux is an upper limit to the infrared core source, since no counterpart to this source is seen shortward of 1.3 μm. The solid line is a modified blackbody function with $T = 300$ K fitted to the infrared SED. The dashed lines show a radiation transfer model of the complete SED with three components: dust reradiation accounting for the infrared, bremsstrahlung from cooling gas dominating the UV to X-ray regime, and synchrotron emission dominating the radio flux.

The radio data, although of low spatial resolution, are dominated by the Circinus nucleus but certainly include extended emission from the lobes (Elmouttie et al. 1995); the nuclear X-ray emission is resolved by *Chandra* into various pointlike sources surrounding a bright source that is associated with the nucleus. These satellite sources have 2–10 keV unabsorbed luminosities in the range 10^{37}–10^{40} ergs s^{-1} (Smith & Wilson 2001; no luminosity is provided for the nuclear source), from which we infer that the more than 1 order of magnitude flux found by *BeppoSAX* originates mostly from the nuclear source.

The most prominent feature in the SED is a narrow peak at infrared wavelengths, indicative of dust emission in a narrow temperature range. This peak is well approximated by a simple modified blackbody function with a temperature of about 300 K (Fig. 4, *solid line*). Dereddening for extinctions up to $A_V = 20$ (see below) does not really modify the dust temperature, mainly because of the steep shape of the infrared SED. Additional components of cooler dust may be present (this dust is not traced by our data), but hotter dust is not detected; it either is not present or is totally extincted. Some excess emission over the modified blackbody is apparent at 2.2 μm and below, but that may be a result of a combination of the underlying galaxy contribution and bremsstrahlung emission from cooling gas, both of which could still contribute to these small apertures. Also in Figure 4, we show a model of the complete radio to X-ray SED using the SUMA code (Contini et al. 2004 and references therein). Briefly, this code considers the coupling effect of photoionization from an external source (the AGN, in this case) and shocks into an ensemble of clouds randomly distributed around the AGN and characterized by different physical conditions of shock velocities, preshock densities, preshock magnetic field, cloud geometrical thickness, and dust-to-gas ratios. As a preliminary result, we find the current nuclear SED to be characterized by shock-dominated clouds. The infrared to X-ray SED can be simultaneously fitted by shock-dominated clouds with velocities $\gtrsim$1000 km s^{-1} and downstream densities $n_e = 10,000$ cm^{-3}. Both ranges of values are compatible with what one would expect at radii of a few parsecs from the center. Accordingly, the infrared bump is dominated by dust reradiation from clouds with those velocities while the X-ray to UV regime is dominated by bremsstrahlung. The radio

emission is pure synchrotron radiation generated by the Fermi mechanism at the shock front. No radiation-dominated clouds appear in this model. Since they must exist, their absence is interpreted as an indication that heavy obscuration is occurring at distances of less than 1 pc from the nucleus. We note that the contribution of these high-velocity clouds to the nebular spectrum is negligible, as found by Contini et al. (1998). These clouds are located very close to the center and at most will contribute to the production of coronal and He II lines. Indeed, new high-resolution spectra of optical and infrared coronal lines of Circinus reveal line widths with $V \sim 400$ km s^{-1}, whereas the average nebular line width measured in this galaxy is only 100 km s^{-1} (Rodriguez-Ardila et al. 2004). Independent evidence for the existence of high-velocity clouds is provided by the maser outflow velocities of $V \sim 400$ km s^{-1} measured at less than 0.1 pc from the center (Greenhill et al. 2003). Larger maser velocities may be present, but a wider VLBI velocity baseline would be needed to probe them.

Beyond the nuclear region of Circinus, the effect of dust obscuration is best illustrated by the [$J-2.42$ μm] color image shown in Figure 3 (a [$J-K_s$] color image shows exactly the same structure, but the 2.42 μm image is preferred because it includes only continuum emission). Figure 3 shows a patchy distribution of bright and dark regions, with the brighter regions located mostly toward the southeast side of the galaxy. These brighter regions correspond to stronger K_s-band emission and spatially correlate with the darker zones seen, for example, in the F814W and J-band images (Fig. 1). Thus, they probably mark the location of cooler dust. Further comparison of the F814W and [$J-2.42$ μm] images reveals that this cool dust follows well-defined channels that seem to spiral down toward the center.

Comparison of the [$J-2.42$ μm] colors at different points in the galaxy to average values in normal ellipticals ($J - K = 0.95$; Giovanardi & Hunt 1996) leads to extinction estimates in the range $A_V = 2-6$ mag (for a foreground screen) or 6–20 mag (if the dust and stars are mixed), depending on position.

At the nucleus itself, the extinction is expected to be much higher, considering the Compton-thick nature of the source. Assuming a standard dust-to-gas ratio, a column density of 10^{24} cm^{-2} translates into an extinction of about 80 at 10 μm, enough to dim any emission from the central source even in the infrared. Since we do in fact see a 2 pc infrared central source, this has to be subject to much less extinction. Considering its size and temperature, and assuming the emission is due to dust reprocessing of radiation from the AGN, the inferred UV luminosity to heat this source is $\sim 7 \times 10^{41}$ ergs s^{-1}. This is within the range of nuclear X-ray luminosities, $L_{2-10\ \mathrm{keV}} \sim 3-17 \times 10^{41}$ ergs s^{-1}, measured from the X-ray spectrum after correction for absorbing columns of 10^{24} cm^{-2}. Thus, the infrared central source in Circinus provides independent support for the Compton-thick nature of its core; it also indicates that any highly obscuring material should be located at distances of less than 1 pc from the core.

We note that the modeling of the SED leads to a different interpretation, viz., that the infrared bump is due to dust heated primarily by shocks, while we found above that the heating of the infrared central source is compatible with direct illumination by the AGN. While both possibilities are perfectly valid, the model is poorly constrained, since the SED is not sufficiently sampled, particularly the millimeter range. For accurate modeling to be accomplished, further X-ray, far-infrared, and millimeter data with resolutions on scales of only a few parsecs are needed.

5. CONCLUSION

The central source of Circinus at infrared wavelengths is resolved in the K_s band as a bright compact region with a FWHM size of 1.9 ± 0.6 pc. This source is only visible at wavelengths longward of 1.6 μm, and it is offset by 0.″15 to the southeast of the brightest central emission seen in the J-band and *HST* optical images. The source is indeed located at the vertex of a rather collimated beam ($\sim$10 pc long) apparent at wavelengths shortward of 1.6 μm. The direction and position of this collimated beam coincides precisely with the main axis of Circinus' Hα ionization cone. No collimation is seen at wavelengths beyond the K_s band. As scattering is more effective at shorter wavelengths, the observed feature may be nuclear light scattered by the compact dusty structure in which the Circinus nucleus seems to reside.

The source also coincides with the peak of the [Si VII] 2.48 μm line emission and with the center of a 19 pc extended [Si VII] bicone of ionized gas. On the basis of the arguments above, the infrared source that has been detected can be associated with the nucleus of Circinus.

The astrometric position of the infrared source differs by at least 0.″3 in declination from the VLBI maser position. While this may be because of a systematic difference between the radio and optical/infrared reference frames, an alternative possibility is that the maser source is related not to the nucleus but instead to the outflowing material traced by the VLBI data.

The size of the infrared central source is compatible with a putative parsec-scale torus. Its SED can be fully accounted for by dust at about 300 K, and the required AGN luminosity to heat such dust at a distance of 1 pc from the core is in the range of luminosities derived from X-ray data. This energy balance implicitly supports the presence of column densities as high as 10^{24} cm^{-2} at the nucleus. The absorbing material has to be located at distances within 1 pc of the core and be rather inhomogeneously distributed in order for the dust at 300 K to have a direct view of the AGN. Hotter dust is not detected at distance scales of 2 pc; it is either not present or is heavily extincted. Additional cooler gas may certainly be present, probably distributed at slightly larger radial scales. This cold dust is not sampled by our data, but interferometric data at millimeter wavelengths should probe this regime in the future.

Within a 200 pc radius of the central source in Circinus, the extinction derived from color maps is inhomogeneous, with $A_V = 2-6$ mag depending on position. Close to the central source, higher extinctions of $A_V = 6$ mag (for a foreground screen) or $A_V = 20$ mag (if the dust and stars are mixed) are found.

REFERENCES

Brinkmann, W., Sibert, J., & Boller, T. 1994, A&A, 281, 355
Contini, M., Viegas, S. M., & Prieto, M. A. 1998, ApJ, 505, 621
———. 2004, MNRAS, 348, 1065
Elmouttie, M., Haynes, R., Jones, K., Ehle, M., Beck, R., & Wielebinski, R. 1995, MNRAS, 275, L53
Freeman, K. C., Karlsson, B., Linga, G., Burrell, J. F., van Woerden, H., & Goss, W. M. 1977, A&A, 55, 445
Giovanardi, C., & Hunt, L. K. 1996, AJ, 111, 1086
Greenhill, L. J., Kondratko, P. T., Lovell, J. E. J., Kuiper, T. B. H., Moran, J. M., Jauncey, D. L., & Baines, G. P. 2003, ApJ, 582, L11

Maiolino, R., Alonso-Herrero, A., Andres, S., Quillen, A., Rieke, M., Rieke, G. H., & Tacconi-Garman, L. 2000, ApJ, 531, 219
Marconi, A., et al. 1994, Messenger, 78, 20
Matt, G., et al. 1999, A&A, 341, L39
Quillen, A., et al. 2001, ApJ, 547, 129
Rodriguez-Ardila, A., Prieto, M. A., & Viegas, S. 2004, in IAU Symp. 222, The Interplay among Black Holes, Stars and ISM in Galactic Nuclei, preprint (astro-ph/0406648)
Smith, D. A., & Wilson, A. S. 2001, ApJ, 557, 180
Wilson, A. S., Shopbell, P. L., Simpson, C., Storchi-Bergmann, T., Barbosa, F. K. B., & Ward, M. J. 2000, AJ, 120, 1325